Available online at www.sciencedirect.com
ScienceDirect
Cement and Concrete Research 37 (2007) 264–269
Cement and Concrete Research

Fatigue behavior of a multi-scale cement composite

Edouard Parant *, Pierre Rossi, Claude Boulay

Laboratoire Central des Ponts et Chaussées, Paris, France

Received 16 June 2004; accepted 2 April 2006

Abstract

To conceive structural elements with a cement composite and without any reinforcement except steel fibers is a very exciting and difficult challenge, which can change the building construction fields. To achieve this objective the Laboratoire Central des Ponts et Chaussées (LCPC) has developed a new cement composite, CEMTEC$_{multiscale}$®, which is strain hardening in tension and has a very high uniaxial tensile strength, more than 20 MPa.

The present paper is on an experimental research related to this composite fatigue behavior. The principal results obtained are the following:

– A strong correlation exists between the initial static damage and the fatigue endurance limit.
– Below a loading ratio $R=0.65$ (ratio between the applied stress and the characteristic static stress), failure during bending fatigue tests never appears with CEMTEC$_{multiscale}$® specimen.
– An 8% gain is observed between the bending static behavior of the specimens being previously loaded in fatigue and those not being loaded in fatigue.

Keywords: Fatigue; Composite; Multi-scale reinforcement; Bending strength; Ultra high-performance concrete

1. Introduction

For a few years the Laboratoire Central des Ponts et Chaussées (LCPC) has worked on the development of new cement composites. These materials are the direct implementation of the "Multi-Scale Concept" developed by Rossi [1]. The idea is to mix short fibers with longer fibers in order to intervene at the same time on the material scale (increase of the tensile strength) and on the structure scale (bearing capacity and ductility). A Multi-Scale Cement Composite (MSCC) is then obtained. As an example, a MSCC was developed in the past [2] constituted by a mix of 5% of straight cylindrical fibers (made of drawn steel) of 5 mm length and of 0.25 mm in diameter and of 2% of cylindrical hooked fibers (made of drawn steel) of 25 mm length and of 0.3 mm in diameter. The uniaxial tensile behavior of this MSCC is strain hardening and its average tensile strength is about 15 MPa. The new MSCC, called CEMTEC$_{multiscale}$®, which was the subject of a world patent filling by the LCPC in March 2001, is elaborated like a MSCC, but with some evolutions:

– Whereas the previous MSCC contains 2 different metal fiber geometries, the new one contains 3 of them [3];
– This MSCC contains 11% per volume of fibers whereas the previous one contains 7% of them.

Table 1
Mix design of the CEMTEC$_{multiscale}$®

Raw materials		Quantities	
OPC	(CPA CEM I 52.5 R)	1050	kg/m^3
Sand	(Quartz 125–400 μm)	514	kg/m^3
Silica fume	(Zirconium)	268	kg/m^3
Superplastizer	(Polyphosphonate — 30%)	44	kg/m^3
Total water		211	liter
Steel fiber content		897	kg/m^3
Silicate fume/cement	0.255	Superplat/Liant	1.02%
Sand/cement	0.573	Air void	2%
Water/cement	0.201	Specific gravity	2.98
Water/binder	0.16	fc [MPa]	220

* Corresponding author. LCPC-58, Boulevard Lefebvre — 75732 Paris Cedex 15, France. Tel.: +33 1 40 43 52 95; fax: +33 1 40 43 54 98.
E-mail address: eparant@yahoo.fr (E. Parant).

0008-8846/$ - see front matter © 2006 Elsevier Ltd. All rights reserved.
doi:10.1016/j.cemconres.2006.04.006

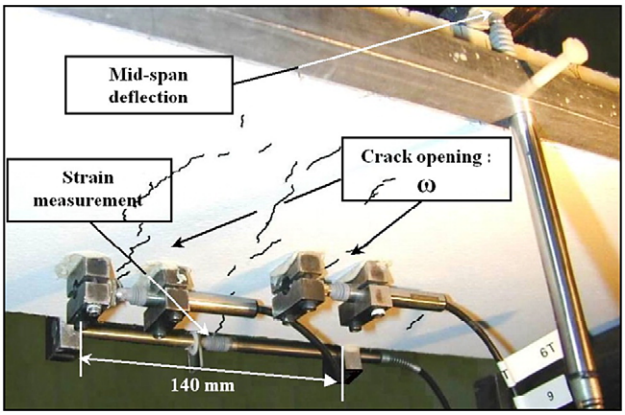

Fig. 1. Four point bending test set-up — example of instrumentation.

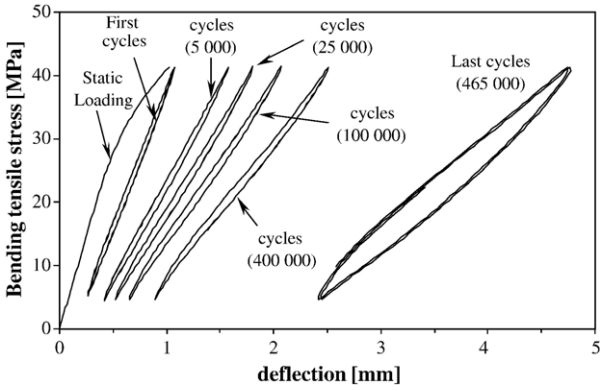

Fig. 3. Cyclic stress–deflection curves until rupture.

In 2000, the LCPC launched a vast study over 4 years on CEMTEC$_{multiscale}$®, which comprised tests to characterize the various mechanical behaviors of the composite (static and fatigue behaviors [4], high strain rate loading effect), tests of durability [3], tests on structural elements, and tests to optimize the manufacturing process (mixing and casting).

2. Research significance

The new cement composite has been developed to be stress hardening in tension and to have a very high tensile strength, more than 20 MPa [5]. It should be underlined that the industrial applications mainly for this new composite relates to "2D" prefabricated structures like thin structural slabs or shells without any reinforcement except steel fibers. So, it is very important, if we consider these industrial applications, to know and to quantify the fatigue behavior of the composite studied material. The present paper is on an experimental research related to the MSCC fatigue behavior.

3. Mix design, casting and curing procedures

The composition of CEMTEC$_{multiscale}$® is given in Table 1. The specimens are cast flat, in three successive layers, on a vibrating square plate. The specimens have a 600 mm length, a 200 mm width and a 40 mm thickness. The 200 mm width allows an orthotropic orientation of the fibers representative of what happens in a real slab. The longest reinforcement is composed by end hooked fibers, which are 25 mm length. This fiber geometry improves significantly endurance limit [6]. It is known that with every law water/binder ratio matrix, as for the studied MSCC, the use of heat treatment makes it possible to increase matrix mechanical performances [7,8]. So, specimens were placed in a drying oven at 90 °c during 4 days, 48 h after their release from the mould. Finally, for each specimen, the upper face was ground to obtain a constant thickness and inertia.

4. Mechanical tests

Twenty-four specimens were fabricated. The age of all the specimens is of more than 10 months at the beginning of the tests. In a first time, 9 specimens from a series of 24 were tested in a 4-point static bending test. The test is carried out at an imposed deflection rate equal to 0.2 mm/min. During these bending tests, the distance between the supports is 420 mm for lower supports and 140 mm for the higher supports. The deflection is measured using a special extensometer [9], placed on the specimens, designed to eliminate vertical parasitic displacements on the level of the supports. A second LVDT

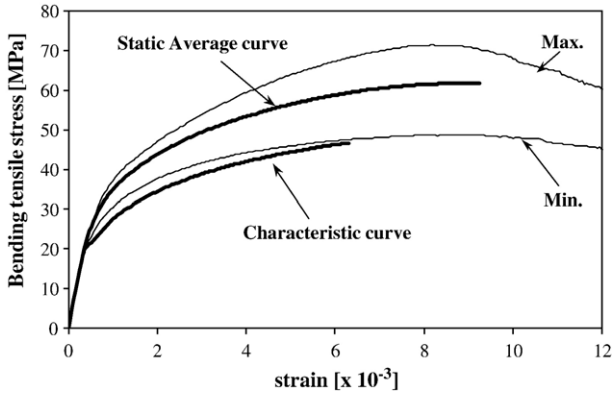

Fig. 2. Static bending tensile stress–strain curves.

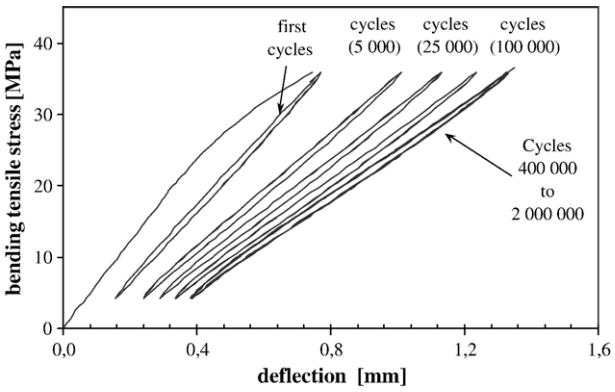

Fig. 4. Cyclic stress–deflection curves with stagnation.

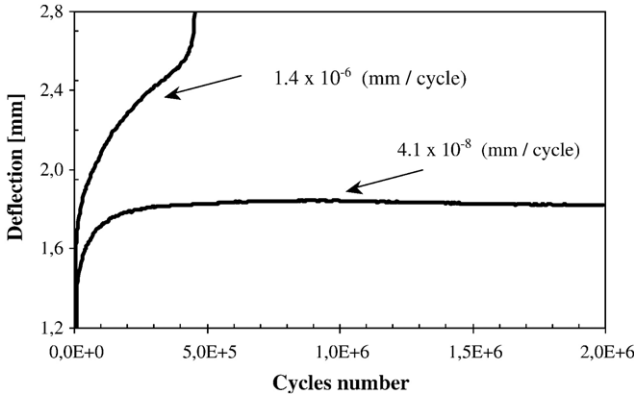

Fig. 5. Deflection evolution–cycle number curves.

transducer is placed at the bottom face of the specimen, in the zone of constant moment, in order to measure the maximal tensile strain.

Then 15 specimens were tested in bending fatigue, at an imposed loading rate (same test set-up than for static tests). A first slow loading rate is imposed to reach the chosen maximal fatigue load. It is important to mention that no visible crack appeared during this stage. Then the load is decreased to reach the average fatigue load and finally the asymmetric sinusoidal fatigue loading is taken between 10 and 100% of the chosen maximal fatigue load. The imposed loading frequency was 2.5 Hz. The test room is a 20 °C air-conditioned room. Tests were led for 2 million cycles (10 days) except in the case of premature failure, in accordance with previous works [6,10]. After the appearance of a visible crack, this was monitored by a transducer. The test set-up related to the static and fatigue loadings is presented in Fig. 1.

Table 2
Fatigue test results

Specimen number	Initial strain ε_i	Slope S	Max. fatigue stress	Loading rate R	Cycle number N_c
	10^{-3}	mm/cycle	MPa		
1	1.04	4.52×10^{-8}	35.9	0.77	2,000,000
2	1.18	2.11×10^{-8}	38.0	0.817	2,000,000
3	1.23	2.09×10^{-8}	36.0	0.77	2,000,000
4	1.25	4.51×10^{-8}	40.7	0.875	2,000,000
5	1.27	4.46×10^{-8}	40.8	0.88	2,000,000
6	1.56	8.47×10^{-7}	41.8	0.90	465,150
7	1.44	9.43×10^{-6}	37.9	0.82	105,898
8	1.79	1.94×10^{-5}	46.5	1.00	41,750
9	1.84	5.93×10^{-5}	48.5	1.04	25,950
10	1.94	2.66×10^{-5}	42.0	0.90	38,620
11	2.10	6.11×10^{-5}	48.3	1.04	23,915
12	2.46	1.46×10^{-4}	49.5	1.06	14,260
13	2.63	4.44×10^{-4}	48.7	1.05	5336
14	2.28	4.3×10^{-4}	46.5	1.00	3260
15	2.86	1.37×10^{-3}	45.0	0.97	1135

5. Test results and discussions

5.1. Static results

Fig. 2 presents the results of the 9 specimens tested in quasi-static condition, and the average and characteristic associated curves. These results are presented in *equivalent tensile stress–strain* curves. The average equivalent bending tensile strength

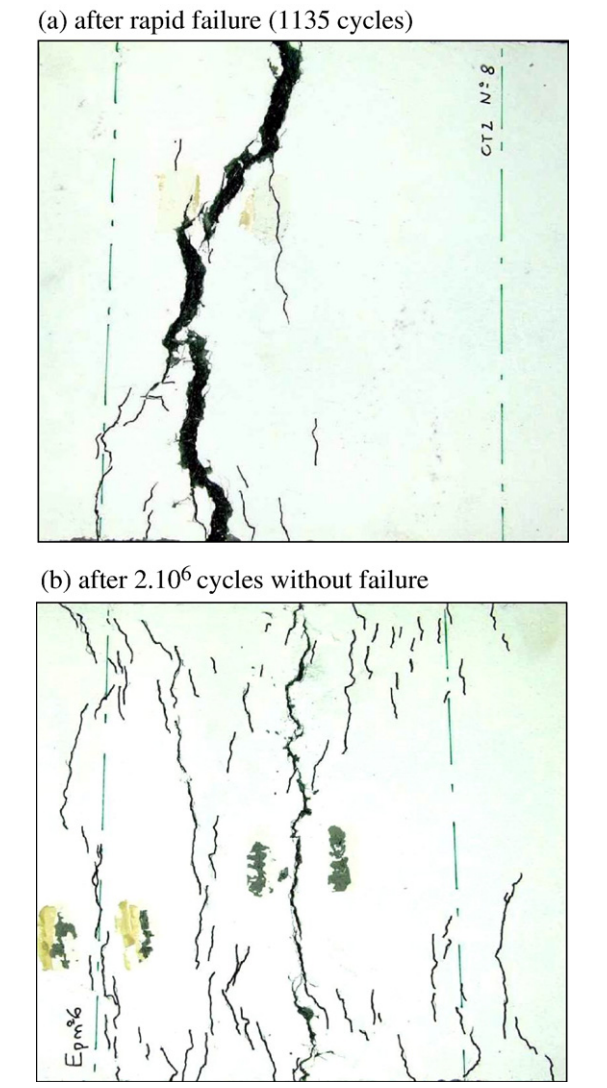

Fig. 6. Cracking patterns of CEMTEC$_{multiscale}$® after fatigue test.

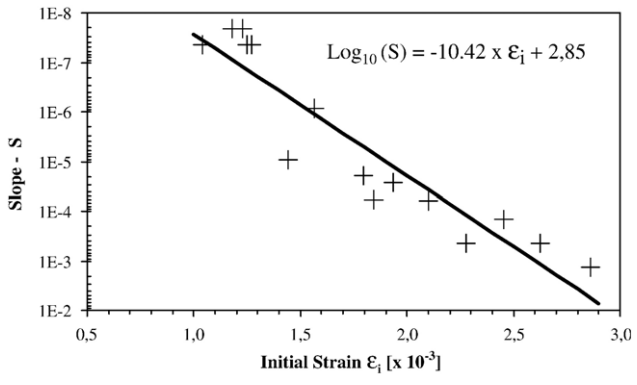

Fig. 7. Deflection evolution slope–initial strain diagram.

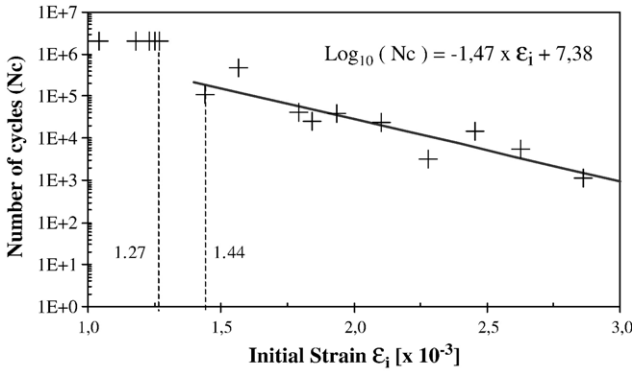

Fig. 8. Initial strain–number of cycles (at rupture) diagram.

Table 3
Reloading after fatigue test, average fatigue results and average static results

Specimen number	Max. fatigue stress (MPa)	MOR (MPa)	Strain ε (10^{-3})	Loading rate R (σ_F/σ_R)	Slope S (mm/cycle)
1	35.9	66.3	2.28 *	0.54	4.52 E−8
2	38.0	66.9	2.59 *	0.57	2.11 E−8
3	36.0	60.2	2.60 *	0.60	2.09 E−8
4	40.7	65.3	3.38 *	0.62	4.51 E−8
5	40.8	74.3	2.80 *	0.55	4.46 E−8
Fatigue average	–	66.6	2.73 *	0.58	3.54 E−8
Static average	–	61.5	9.65 **	–	–

*After $2 \cdot 10^6$ cycles and before reloading.
**At rupture for static test.

(called Modulus of Rupture — MOR) is 61.5 MPa (C.O.V.= 0.11) and the corresponding strain is 9.2×10^{-3}.

The determination of the characteristic curve is presented in the Appendix.

5.2. Fatigue results

During the study, the loading ratio R (ratio between the applied stress and the characteristic static stress) varied between 0.77 and 1.03.

In Figs. 3 and 4 are presented examples of fatigue bending tensile stress–deflection curves respectively related to a specimen which has failed before 2 million cycles and to a specimen which has not failed. In the Fig. 5 are presented examples of *deflection–cycles number* curves respectively related to the case where the specimen is broken before 2 million cycles and the case where the 2 million cycles were reached. We find the usual shape of the fatigue curves with three different phases:

- A first phase, corresponding to a starting micro-cracking of the matrix. The deflection evolution is fast.
- A second phase marked by a deflection evolution slowing down.
- A third phase, which marks the resumption of the damage and leads very fast to the ruin of the structure. This last one is of course absent for specimen weakly damaged.

In Fig. 6 are presented the cracking patterns of two specimens; the first one is obtained after a rapid rupture (1135 cycles) and the second one after $2 \cdot 10^6$ cycles (no failure). It is clear that a rapid deflection evolution leads to a poor density of cracks, and then to a concentration of stress in a narrow area. On the contrary, a moderate deflection evolution leads to a diffuse multiple cracking, induced by multi-scales reinforcement efficiency. That gives time to pseudo-accommodation of the MSCC specimen; in that case, the maximum crack opening amplitude does not exceed 100 μm and no rupture happened during the fatigue test.

In Table 2 are presented the principal fatigue test results. By looking at the last three columns (*fatigue stress*, *load ratio* and *cycles number*), one can make the following remarks:

- Results are relatively scattered, that is usual for fatigue tests;
- Below a loading ratio $R=0.82$, MSCC specimens do not fail by fatigue before 2 million cycles.

The scattering observed in Table 2 indicates that the applied load ratio is not a good parameter to analyze the fatigue failure probability of this material. The applied stress/MOR ratio related to each specimen is surely a better parameter to evaluate this fatigue failure probability of a specimen. But it is impossible to determine this ratio, since the MOR of each specimen is

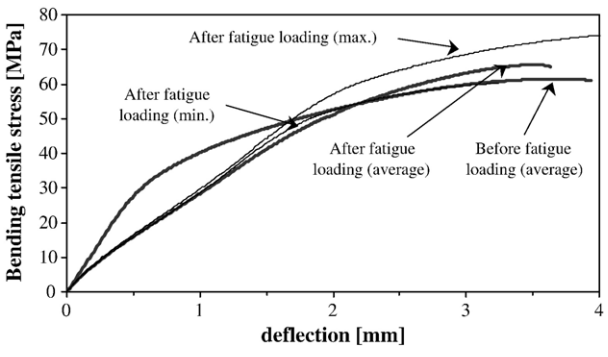

Fig. 9. Static behavior before and after fatigue loading.

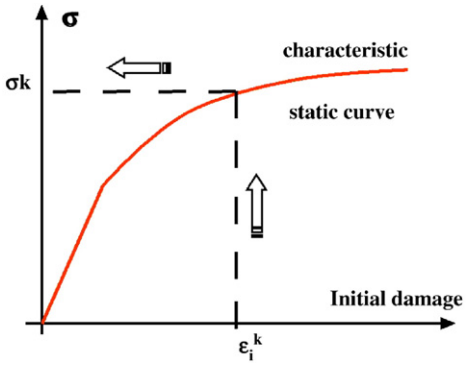

Fig. 10. Initial damage and corresponding stress.

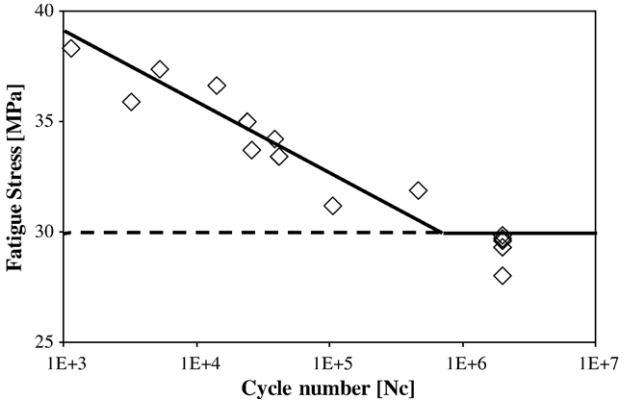

Fig. 11. Corrected Wöhler curve — endurance limit.

unknown. The initial static damage (quantitatively represented by the initial static strain ε_i) generated during the first static load could be a better parameter to evaluate this fatigue failure probability. To show this dependence, the relation between S, the derivative of deflection evolution-cycles number curve, and the initial static strain, is considered. The rate S is known to be a good indicator of the fatigue lifetime [10–12]. It is observed a good correlation between the stationary fatigue damage phase, represented by S, and the initial static damage ε_i, as shown in Fig. 7. Considering this positive result, the *fatigue failure cycles number–initial strain* diagram can be drawn (Fig. 8). We remark that:

- There is a critical initial strain threshold, below which specimens do not break before 2 million cycles, while beyond this threshold the rupture becomes inevitable. This threshold value is between 1.27×10^{-3} and 1.44×10^{-3}.
- Beyond the threshold, there is a linear relation between the fatigue failure cycles number and the initial static strain.

Specimens having reached the 2 million cycles were then reloaded in quasi-static test until rupture. Fig. 9 presents the average static reloading curve, as well as the average static curves (i.e. before and after 2 million fatigue cycles). For more legibility, we incorporate the min and max reloading static curves. The global results are given in Table 3. We can observe that the static bending behavior after 2 million fatigue cycles is better than those related to the specimens not loaded in fatigue. This confirms some previous studies [6,13,14], which mention that a low loading ratio is beneficial for the residual strength of FRC beam. The gain is about 8% and the authors propose some explanations with a fracture mechanic approach in [3]. The deflection at the strength peak is approximately the same in the two curves.

To conclude this study, we tried to calculate an endurance limit. Knowing the static characteristic curve (Fig. 2) and each initial strain ε_i^k (Table 2), we can determine the corresponding stress for all specimens tested in fatigue (Fig. 10). Then one determines a corrected Wöhler curve linking fatigue stress and cycle number (Fig. 11). Finally, if we consider the characteristic stress related to a strain equal to 1.27×10^{-3}, which is the lower value of the critical initial strain evocated above, we obtain a characteristic stress equal to 30 MPa, that corresponds to a loading ratio R of 0.65.

6. Conclusions

A new ultra-high performance cement composite, the CEMTEC$_{multiscale}$®, was tested under asymmetric fatigue loading. From this experimental study, the following comments can be made:

1. The stationary damage fatigue evolution of a specimen is dependent on the initial static damage of this specimen. It is also possible to predict fatigue life only with the knowledge of the initial static strain (i.e., obtained during a first slow loading rate).
2. A critical initial static strain threshold exists. The strain threshold determined in this study is between 1.24×10^{-3} and 1.44×10^{-3}. Below this threshold, no failure occurs during the bending fatigue test and beyond this threshold the number of cycles to failure linearly depends on the initial static strain.
3. Expressed in terms of a loading ratio R, failure during fatigue test never appears when $R\leq0.65$. The corresponding bending tensile strength is equal to 30 MPa.
4. A gain of 8% is observed between the bending static behavior of the specimens being previously loaded in fatigue, and those not being loaded in fatigue.

Acknowledgements

The authors thank the team of S. Ricordel, namely J.D. Simitambe, F. Guiradot and J. Carriat for the important work supplied during the mixing operations and preparation of specimens.

Appendix A

The characteristic curve of static tests is determined in the following way:

1. One distinguishes for all individual curves a linear elastic part and a nonlinear part. To distinguish between these two parts, one traces their derivative compared to the X-coordinate, for all the individual curves. Thus one obtains curves with a portion quasi-constant on the left side, and a non-constant portion according to the X-coordinate. The border between these two curve portions constitutes the limit of the linear elastic field of the primitive curve.
2. One determines then the linear part of the characteristic curve in the following way:
   - For the slope of the curve one takes the average slope.
   - For the limit of the linear part, one takes the average limit (obtained with the average curve) less $k(n)\times$*standard deviation on this limit* (obtained starting from the individual curves). $k(n)$ is the Student coefficient for a 5% fractile and then depends on the number n of tests carried out (thus the curves taking part in the analysis).

3. One determines then the nonlinear part of the characteristic curve in the following way:
   – First of all, one calculates the characteristic value related to the modulus of rupture as following: $R_{char.} = R_{aver.} - k(n) \times s(R)$, where $R_{aver.}$ is the average rupture modulus value and $s(R)$ the standard deviation on this value, $k(n)$ being the Student coefficient for a 5% fractile.
   – Then one multiplies, for each average curve strain value, the corresponding stress by the $R_{char.}/R_{aver.}$ ratio. Thus one plots a characteristic curve up to the characteristic strain value.

References

[1] P. Rossi, P. Acker, Y. Malier, Effect of steel fibers at two stages: the material and the structure, Materials and Structures 20 (1987) 436–439.

[2] P. Rossi, High performance multi-modal fiber reinforced cement composite (HPMFRCC): the LCPC experience, ACI Materials Journal 94 (6) (1997) 478–483.

[3] E. Parant, "Mécanismes d'endommagement et comportements mécaniques d'un composite cimentaire fibré multi-échelles sous sollicitations sévères: fatigue, choc, corrosion ", PhD from ENPC, Paris, France, 2003, 248 p., in French. (http://pastel.paristech.org/archive/00000507/).

[4] E. Parant, P. Rossi, C. Boulay, Mechanical behavior of a new ultra high performance cement composite under plastic fatigue loading, Proceedings of the *fib* 2003 Symposium, May 6–8, Athens, Greece, 2003, pp. 174–175.

[5] C. Boulay, P. Rossi, J.L. Tailhan, Uniaxial tensile test on a new cement composite having a hardening behavior, Proceedings of the Sixth RILEM Symposium on Fiber Reinforced Concrete (FRC) (BEFIB 2004), 20–22 September 2004, Varenna-Lecco, Italy, 2004.

[6] V. Ramakrishnan, et al., Cyclic behavior, fatigue strength, endurance limit and models for fatigue behaviour of FRC, in: A.E. Naaman, H.W. Reinhardt (Eds.), Proceedings of the 2nd International RILEM Workshop: High Performance Fiber Reinforced Cement Composites 2 (HPFRC 2), 1995, pp. 103–116.

[7] P. Richard, M. Cheyrezy, Les bétons de poudres réactives, Annales de l'ITBTP 532 (1995) 85–102 (in French).

[8] H. Zanni, M. Cheyrezy, V. Maret, S. Philippot, P. Nieto, Investigation of hydration and pozzolanic reaction in reactive powder concrete (RPC) using ^{29}Si NMR, Cement and Concrete Research 26 (1) (1996) 93–100.

[9] C. Boulay, A. Colson, A concrete extensometer eliminating the influence of transverse strains on the measurement of longitudinal strains, Materials and Structures 14 (1981) 35–38.

[10] M.K. Lee, B.I.G. Barr, An overview of the fatigue behavior of plain and fiber reinforced concrete, Cement and Concrete Composites 26 (4) (2004) 299–305.

[11] BEFIM, Le Développement Industriel des Bétons de fibres Métalliques, Conclusions and Recommendations from the French National Project — Civil Engineering Plan, Presse de l'Ecole Nationale des Ponts et Chaussées, Paris, France, 2002, 262 pages, (in French).

[12] D. Mouquet, G. Bernier, M. Behloul, Etude du comportement à la fatigue du BPR fibré, Proceedings of the 5th International RILEM Symposium: Fibre-Reinforced Concretes (FRC) BEFIB'2000, P. Rossi & G. Chanvillard edition, Lyon, France, 13–15 September 2000, 2000, pp. 769–780, (in French).

[13] A.E. Naaman, H. Hammoud, Fatigue characteristics of high performance fiber-reinforced concrete, Cement and Concrete Composites 20 (1998) 353–363.

[14] V. Ramakrishnan, G. Orberling, P. Tatnall, Flexural fatigue strength of steel fiber reinforced concrete, Fibre Reinforced Concrete—Properties and Applications, SP 105-13, ACI, Detroit, 1987, pp. 225–245.